ACS APPLIED MATERIALS & INTERFACES

Research Article

www.acsami.org

Controllable Fabrication of Noniridescent Microshaped Photonic Crystal Assemblies by Dynamic Three-Phase Contact Line Behaviors on Superhydrophobic Substrates

Jinming Zhou,*[,†] Jing Yang,[†] Zhandong Gu,[†] Guofu Zhang,[†] Yu Wei,[†] Xi Yao,[§] Yanlin Song,[‡] and Lei Jiang[‡]

[†]Key Laboratory of Inorganic Nanomaterials of Hebei Province, College of Chemistry and Material Science, Hebei Normal University, Shijiazhuang, 050024 P. R. China

[‡]Key Laboratory of Green Printing, Key Laboratory of Organic Solids, Institute of Chemistry, Chinese Academy of Sciences, Beijing, 100190 P. R. China

[§]Department of Biomedical Sciences, City University of Hong Kong, Tat Chee Avenue, Kowloon, Hong Kong

Supporting Information

ABSTRACT: Enormous research efforts have been made to self-assemble monodisperse colloidal spheres into special microscopic shapes (e.g., superbeads, superballs, or doughnuts), due to their widespread applications in sensors, displays, separation processes, catalysis, etc. But realization of photonic crystal (PC) assemblies with both facile microshape control and a noniridescent property is still a tough task. Herein, we demonstrate the controllable fabrication of noniridescent microshaped PC assemblies by evaporation-induced self-assembly inside aqueous colloidal dispersion droplet templates on superhydrophobic substrates. The microshapes of the PC assemblies could be tuned from microbeads to microwells to microellipsoids by manipulating the dynamic behaviors of the three-phase contact line of the colloidal droplets during the evaporating process. Structure characterization shows that the PC assemblies are crack-free, consisting of an ordered periodic arrangement of colloidal spheres in the surface layers and amorphous inner layers. The incorporation of black Fe_3O_4 nanoparticles into the PC assembly lattice is demonstrated to endow the PC assemblies with enhanced noniridescent structural colors with wide-viewing angles and a superparamagnetic property. The crack-free noniridescent PC assemblies with controlled microshapes have promising applications in the fields of nontoxic, nonbleaching pigments and energy-efficient full-color display pixels, and their facile fabrication procedure may provide guidance for creating new types of substructured colloidal particles.

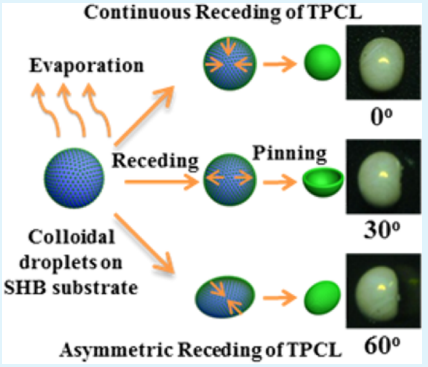

KEYWORDS: *photonic crystals, superhydrophobic substrates, structural colors, microshapes, noniridescence*

INTRODUCTION

Self-assembly of monodisperse colloidal microspheres into periodic crystalline arrays is an effective tool for development of novel functional materials. Ordered crystalline structures at optical wavelength may possess a photonic band gap in the visible region, within which certain frequencies of light could be forbidden.[1,2] These special optical materials, called photonic crystals (PCs), have already found applications in optical communications,[3,4] full-color displays,[5,6] sensors,[7−9] and other optical devices.[10−13] Besides the great achievements in improving the assembly quality of PCs, mainly in the form of thin films for their practical applications,[14−17] considerable attention has also been paid to the development of various special microshaped opal or inverse opal structured assemblies, for instance, balls (or beads),[18−26] eyeballs,[27] doughnuts,[28] boats,[29] and others,[30] for the pursuit of novel optical properties.

The fabrication approaches for highly ordered microshaped assemblies from colloidal spheres could be mainly categorized into two types based on the nature of the assembly environment: the wet-assembly method in a liquid media and the dry assembly method on a solid substrate. The conventional wet-assembly method utilizes water-in-oil emulsions as the assembly units with the suspending spherical water droplets containing monodisperse colloids in the oil phase acting as the assembling templates (or, in certain cases, the functional materials are in the oil phases and undergo self-assembly at the oil−water interface), which guides the assembly of the monodisperse spheres or other functional materials into the final desired microshapes.[18−25,27,31−33] However, a final drying process to remove the oil phase (usually a dense, toxic, fluorinated oil) is needed, which prolongs the fabrication process and may bring environmental problems. For the dry

Received: August 12, 2015
Accepted: September 21, 2015
Published: September 21, 2015

DOI: 10.1021/acsami.5b07443
ACS Appl. Mater. Interfaces 2015, 7, 22644−22651

assembly method, aqueous colloidal droplets on solid substrates are dried under ambient atmosphere and the colloidal spheres in the droplet self-assemble into interesting microshapes. Obviously, the dry-assembly method exhibits more advantages by avoiding the use of the oil phase and simplifying the fabrication process. The "coffee ring" left behind from a spill of coffee on a hydrophilic solid substrates is a convenient example of the dry-assembly method.[34] When hydrophobic or superhydrophobic (SHB) substrates are used, the self-assembled microshapes are quite different. Contrary to the ringlike relics on hydrophilic substrates, colloidal supraballs, soccer balls, or "doughnut" were fabricated by dispensing aqueous colloidal droplets with controlled colloidal concentrations onto SHB substrates and drying under ambient conditions;[26,28,35] PC domes or hemispheres were fabricated on hydrophobic substrates with contact angles of 93°−100°.[36,37] However, the structural colors of the above-mentioned assemblies were usually angle-dependent, due to Bragg's diffraction of their periodic structures,[18,19,26,28] hindering their practical applications in fields of pigments or display pixels requiring unvarying colors with wide-viewing angles. There lacks an efficient control over the microshapes (usually in the form of balls) of the PC assemblies possessing noniridescent structural colors,[22−25] which is not qualified for applications in areas where asymmetry is inevitable; thus, it is still a great challenge to control the microshapes of the PC assemblies with noniridescent structural colors efficiently by the facile dry-assembly method on SHB substrates, especially to fabricate the more interesting asymmetric assemblies.

In this work, we developed a facile and highly controllable dry-assembly method for fabrication of PC assemblies with noniridescent structural colors by evaporation-induced self-assembly inside aqueous colloidal droplet templates on SHB substrates. The different dynamic behaviors (receding or pinning) of the three-phase contact line (TPCL) of the aqueous colloidal droplets evaporating on SHB substrates accounted for PC assemblies with varying microshapes from microbeads to asymmetric microwells and microellipsoids. Structure characterization shows that the PC assemblies are crack-free, which possess face-centered cubic periodicity in the surface layer and amorphous arrangement in the inner layers. The incorporation of black Fe_3O_4 nanoparticles into the lattice of this unique structure was demonstrated to be able to endow the PC assemblies with enhanced noniridescent structural colors, based on the combined effects of the spectrally resonant scattering of the ordered surface layers, the single scattering process with wavelength-specific constructive interference of the inner amorphous photonic structures, and the curvature of the surface. Uniform incorporation of black Fe_3O_4 nanoparticles without affecting the structures of the PC microassemblies renders them superparamagnetic, and the colored PC assemblies could be moved and collected by an external magnetic field. The special microshaped noniridescent superparamagnetic PC assemblies have promising applications in fields of nontoxic, nonbleaching pigments and full-color display pixels, and the facile fabrication procedure may provide guidance for creating new types of substructured colloidal particles. The results are also relevant to the control of the drop shapes in inkjet printing.

EXPERIMENTAL SECTION

Fabrication of Noniridescent Microshaped PC Assemblies. Poly(styrene−methyl methacrylate−acrylic acid) [P(St-MMA-AA)] colloidal particles with sizes of 184, 210, and 265 nm were synthesized by one-step emulsion polymerization using our previous method[38] and were directly used without further purification. The weight content of colloids (in the range of 10−20 wt %) was determined before use. To obtain colloidal dispersion with higher colloid contents, the as-prepared aqueous colloidal dispersion was evaporated at 40 °C with stirring to let the proper amount of water escape away. The colloidal droplets with colloidal concentrations of 5−50 wt % and volumes of 0.2−2 μL were dispensed by a 10-μL microsyringe onto SHB substrates and dried at a temperature of 25 ± 1 °C. The SHB substrates were fabricated by coating the glass slides with a solution (1 g in 30 mL of chloroform) of polydimethylsiloxane-modified silica nanoparticles (average 14 nm).[39] Fe_3O_4 nanoparticles with sizes of about 15 nm, which was added to the colloidal droplets to enhance the structural colors of the PC assemblies, were synthesized by a coprecipitation of ferric and ferrous salt at a constant pH value of 9 under N_2 atmospheres, according to ref 40. Ethanol and ethylene glycol were used to modify the surface tension of the colloidal droplets for the fabrication of ellipsoidal PC assemblies.

Characterization. The microshapes of the PC assemblies and their top-view formation processes were characterized by an up-right digital optical microscope (Keyence VXH-2000). The side-view formation processes of PC assemblies were recorded by an OCA20 machine (DataPhysics). The digital optical microscopic images of PC assemblies with different viewing angles were obtained by rotating the objective lens of the digital optical microscope (Keyence VXH-2000) while the samples were fixed. The structures of the PC assemblies were characterized by SEM (Hitachi FE-S4800 from our instrumental analytical center) after coating with ∼5 nm of Au via ion sputtering (Hitachi E1045). The reflectance spectra of the PC assemblies were characterized by an HR 4000 fiber optic UV−vis spectrometer in the reflection mode in connection with the digital optical microscope via a 600 μm broadband optical fiber (Ocean Optics Inc., QP600-1-UV/vis) at normal and various incident angles relative to the surface of the sample. A silicon wafer was used as a specular reflectance standard. XRD patterns of Fe_3O_4 nanoparticles were collected on a Bruker AXS D8 Advance X-ray diffractometer using a high-power Cu Kα radiation. The magnetic properties of the samples were measured using a physical properties measurement system (Quantum Design Corp.). The magnetic hysteresis loops of the samples were measured with an applied field of 2 T at 300 K.

RESULTS AND DISCUSSION

Microshape Evolution of PC Assemblies Controlled by Colloidal Concentrations. The PC assemblies were prepared by evaporating the aqueous P(St-MMA-AA) colloidal dispersion droplets (acting as self-assembly templates) dispensed onto SHB substrates, as illustrated in Scheme 1. The SHB substrates with rough structures and a contact angle of ∼151° [Figure S1, Supporting Information (SI)] were used to help produce spherical colloidal droplet templates,[41] in which colloidal self-assembly happened during drying processes. Theoretically, continuous homogeneous receding of the TPCL of the aqueous colloidal droplets evaporating on SHB substrates favors the fabrication of microbead PC assemblies, as illustrated in Scheme 1A. Pinning of the TPCL during aqueous colloidal droplet evaporation could cause the change in the moving directions of the colloidal spheres[34] and may result in the formation of dimpled microbead or microwell PC assemblies (Scheme 1B). Asymmetric receding of TPCL (Pinning in one direction and homogeneous receding in the perpendicular direction) benefits the interesting anisotropic PC assemblies (Scheme 1C). During the evaporation process under an ambient atmosphere, monodisperse P(St-MMA-AA) colloidal spheres[38] with a hard PSt core and soft PAA shell undergo evaporation-induced self-assembly from the outmost aqueous layer, forming a shell of close-packed colloidal spheres

DOI: 10.1021/acsami.5b07443
ACS Appl. Mater. Interfaces 2015, 7, 22644−22651

Scheme 1. Schematic Illustrations of the Microshape Controllable Fabrication of PC Assemblies by Facile Evaporation of Colloidal Droplets on SHB Substrates Based on Different Dynamic Behaviors of the TPCL, Which Is Mainly Determined by Colloidal Droplet Chemical Constitutions: (A) Continuous Receding, (B) Receding and Then Pinning, and (C) Asymmetric Receding of the TPCL[a]

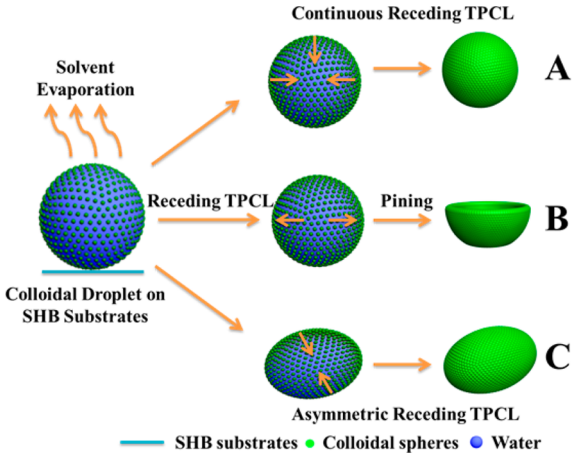

[a]The arrow marks the moving directions of the colloidal spheres inside drying colloidal droplet templates on SHB substrates. (A) Continuous receding of the TPCL of the colloidal droplets on SHB substrate may contribute to the formation of microbead PC assemblies. (B) Receding and then pinning of the TPCL could result in the obtainment of the dimpled or microwell PC assemblies. (C) Asymmetric receding of the TPCL benefits the achievement of the microellipsoidal PC assemblies.

far before complete drying. The hydrogen bonds between the carboxyl groups and the softness of the PAA shell of the monodisperse colloidal spheres ensure their fast and high-quality self-assembly.[42,43]

Investigation of colloid mass fraction increase during the evaporation of water of the aqueous colloidal droplets with varying initial colloid concentrations drying on SHB substrates indicated different evaporation modes (Figure S2, SI). For a high colloidal concentration of 40 wt %, there was a near linear increase in colloid mass fraction in the whole drying process, while for a low colloidal concentration of 10 wt %, the increase in colloid mass fraction indicated two different stages, an almost linear slow increase in the early drying stage and a sharp increase in colloid mass fraction in the late drying stage (Figure S2, SI). The dependence of the evaporation modes on different initial colloid concentrations may originate from the rigidity of the colloid shell formed during the evaporation process on SHB substrates.[28,29] The thicker and more rigid shell for the high colloid concentration helped maintain an even evaporation rate and continuous receding of the TPCL during the whole evaporation process, while the thin shell for low colloid concentration aided the pinning of the TPCL and could be broken by spontaneous buckling due to the pressure gradient across the thin shell,[28,29] resulting in an increase of the evaporation area and the observed increased evaporation rate at the late drying stage (Figure S2, SI). This phenomenon was further evidenced by the following detailed PC assembly formation processes.

The difference in the evaporation modes with different colloidal concentrations may be used to control the microshapes of PC assemblies (Scheme 1). The optical microscopic images of the resultant dried PC assemblies with initial aqueous colloidal droplet volumes of 2 μL and different colloidal concentrations from 5 to 50 wt % are shown in Figure 1 and

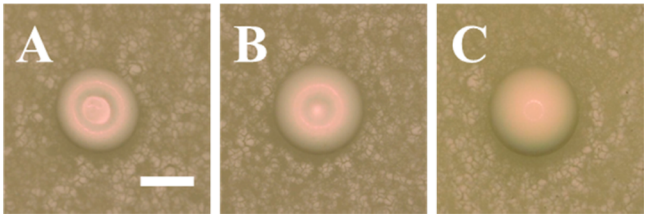

Figure 1. Digital optical microscopic images of the PC assemblies fabricated by evaporating aqueous colloidal droplets with colloidal concentrations of (A) 10 wt %, (B) 20 wt %, and (C) 40 wt % on SHB substrates (scale bar, 800 μm). The microshapes of the PC assemblies evolved from microwells to dimpled microbeads to microbeads with the increase in colloidal concentrations.

the SI (Figure S3). It could be observed that with increasing colloidal concentrations, the shapes of the PC assemblies evolved from microwells (Figure 1A and SI, Figure S3A) to dimpled microbeads (Figure 1B) then to microbeads (Figure 1C and SI, Figure S3B,D). (The mechanism of the success in the PC assembly shape control by different evaporation modes will be discussed in the later section.) We found that drying temperature had little influence on the final shapes of the PC assemblies (Figure S4, SI). The PC assemblies maintained well-like and beadlike shapes for colloidal concentrations of 10 and 40 wt %, respectively, at drying temperatures of 40, 60, and 80 °C (Figure S4, SI), which was due to the insensitivity of the low adhesion and low friction properties of the SHB substrate to temperature.[44] These PC assemblies could be easily detached from the SHB substrates and collected by slightly tapping the SHB substrates, favoring their practical applications.

Formation of Asymmetric Microellipsoidal PC Assemblies Induced by Droplet Surface Tension. Asymmetric PC assemblies are very interesting because of their possible ability to become oriented in external fields (electric or magnetic), which may find applications in optical filters, but their fabrication is always challenging.[29] It is known that the shape of a sessile droplet on a SHB substrate is determined by the bond number $B_o = \Delta\rho g r^2/\gamma$, where $\Delta\rho$ is the difference in the densities of droplet and the surrounding fluid, g the acceleration due to gravity, r the characteristic dimension (in our case droplet radius), and γ is the interfacial tension.[18,28] Obviously, the droplet surface tension plays an important role in determining the shape of the droplets on SHB substrate, which further templates the PC assemblies into desired microshapes upon drying. The increase in bond number with the reduction in colloidal droplet surface tension causes the PC assemblies to deviate from the spherical shape, and asymmetric PC assemblies might be obtained.[18,28]

We chose the water−ethanol system with a well-established surface tension as a model system to investigate the influence of the droplet surface tension on the microshapes of the PC assemblies. Interestingly, microellipsoidal PC assemblies were obtained after drying colloidal droplets (2 μL in volume, 40 wt % colloidal concentration) with 2 vol % ethanol on the SHB substrates in Figure 2A. The major axis of the microellipsoidal PC assembly was ~1552 μm and the minor axis was ~1364 μm (Figure 2A). The aspect ratio is calculated as 1.14. The aspect ratios of the microellipsoidal PC assemblies could be finely tuned by ethanol volume concentrations, with an increase in

DOI: 10.1021/acsami.5b07443
ACS Appl. Mater. Interfaces 2015, 7, 22644−22651

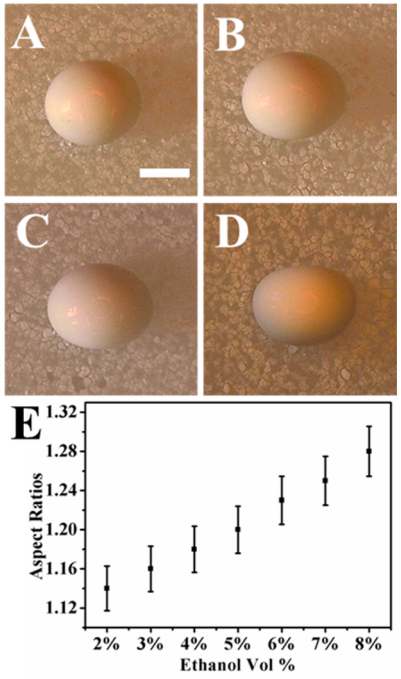

Figure 2. Digital optical microscopic images of PC microellipsoids formed through evaporation-induced self-assembly on SHB substrates by controlling the surface tension of the colloidal droplet templates with varying concentrations of ethanol: (A) 2 vol %, (B) 4 vol %, (C) 6 vol %, and (D) 8 vol %. (E) Dependence of the aspect ratios of the microellipsoidal PC assemblies on the ethanol volume concentrations (scale bars, 800 μm).

the aspect ratio to 1.18 (4 vol %), 1.23 (6 vol %), and 1.28 (8 vol %) for higher ethanol volume concentrations, which could be observed in Figure 2B–E. But when further increasing the ethanol concentration to 10 vol %, microellipsoidal PC boats were achieved (Figure S5A, SI). On the other hand, colloidal droplet volumes (or sizes) had little effect on the aspect ratios of the microellipsoidal PC assemblies. The aspect ratios of PC assemblies fabricated by evaporating colloidal droplets (6 vol % ethanol) with volumes of 0.1–2 μL on SHB substrates were maintained at 1.23 statistically (Figure S5B–D, SI). But the major axes of as-prepared microellipsoidal PC assemblies showed a proportional increase with an increase in colloidal droplet volumes according to $R \propto V^{1/3}$ (Figure S5E, SI), indicating the highly stable evaporation modes of colloidal droplets on SHB substrates. Similarly, ethylene glycol addition could also result in the formation of microellipsoidal PC assemblies but with smaller aspect ratios (Figure S6, SI). This was ascribed to the smaller increase of the bond number due to the corresponding density increase of the colloidal droplets with ethylene glycol addition. The facile fabrication of PC microellipsoids with controlled aspect ratios and sizes has great implications for novel miniaturized optical devices and provides guides for fabrication of miniaturized devices, such as self-reporting miniaturized stirring bars in microreactors.

Formation Processes/Mechanism of PC Assemblies with Controlled Microshapes. The side view and top view of the formation processes of the PC assemblies with controllable microshapes were recorded by an optical contact angle measurement system and digital optical microscope and are shown in Figures 3 and 4. From Figure 3A, the average contact angle of colloidal droplets with 5 wt % of P(St-MMA-AA) colloidal spheres on SHB substrates was ~151°, indicating

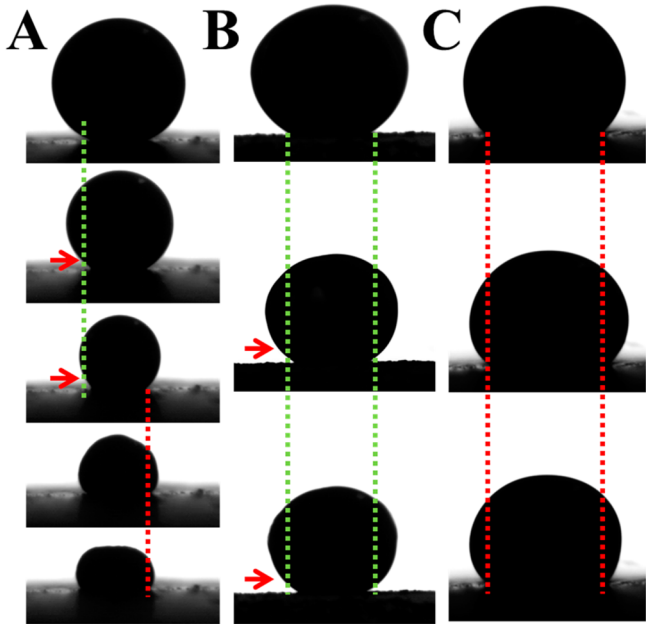

Figure 3. Different evaporation modes of colloidal droplets with colloidal concentration of (A) 5 wt %, (B) 40 wt % without ethanol, and (C) 40 wt % with 2 vol % ethanol recorded by the optical contact angle measurement system at side view. (A) First receding of TPCL in the early stage and then pinning of TPCL in the late drying stages were observed for colloidal droplets with colloidal concentration of 5 wt %. (B) Continuous homogeneous receding of the TPCL in the whole drying stage was observed for droplets with a colloidal concentration of 40 wt %. (C) With the addition of 2 vol % of ethanol into the colloidal droplet with a colloidal concentration of 40 wt %, constant pinning of TPCL was shown during the whole drying process. The dashed lines and arrows are an aid to see the receding or pinning of the TPCL.

the good SHB property of the substrates. With the evaporation of water, the colloidal droplets on SHB substrates demonstrated a continuous receding of the TPCL at the early drying stage and then turned to pinning of the TPCL at the late drying stage (Figure 3A). This observation is in consistent with the top view optical microscopic images of colloidal droplets with the same colloidal concentrations drying on SHB substrates in Figure 4A. At the very beginning, the milky colloidal droplet was spherical because of the SHB property of the substrates (Figure 4A). The milky colloidal droplets turned greenish soon after its dispersion onto SHB substrates (Figure 4A and SI, Supplementary Movie 1), indicating the start of the self-assembly of monodisperse colloidal spheres into ordered structures at the periphery of the droplets due to water evaporation. With the passage of time, the colloidal droplet shrunk homogeneously until 880 s, which is consistent with continuous receding of the TPCL on SHB substrates at an early stage in Figure 3A. Afterward, the sizes of the droplets were almost fixed, corresponding to the stage of pinning of the TPCL in Figure 3A. In this final drying stage, the colloidal spheres flew outward, resulting from the "coffee ring" effects in Figure 4A,[34] contributing to the height changes and dimple development observed in Figure 3A. This final process of TPCL pinning was responsible for the formation of the dimpled or microwell PC assemblies. For droplets with a colloidal concentration of 40 wt % drying on SHB substrates, the static contact angle was still higher than 150°, as is observed in Figure 3B. The TPCL of the colloidal droplets receded

DOI: 10.1021/acsami.5b07443
ACS Appl. Mater. Interfaces 2015, 7, 22644–22651

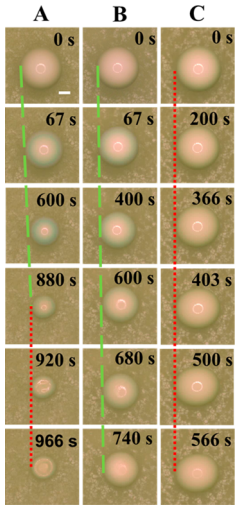

Figure 4. Drying process of colloidal droplets on superhydrophobic substrate with colloidal concentrations of (A) 5 wt %, (B) 40 wt % without ethanol, and (C) 40 wt % with 2 vol % ethanol recorded by top-view digital optical microscope. (A) The colloidal droplets with a concentration of 5 wt % on SHB substrates first shrunk homogeneously from 0 to 880 s, and then the droplets sizes became almost unchanging from 880 s until complete dry. (B) The sizes of the colloidal droplets underwent continuous shrinkage in the whole drying process for colloidal concentration of 40 wt %. (C) With the introduction of 2 vol % ethanol to the colloidal droplet with a colloidal concentration of 40 wt %, the drying colloidal droplets showed asymmetric receding phenomenon. Scale bar, 800 μm. The dashed lines help one to understand the different shrinkage modes during colloidal droplet evaporation on SHB substrates.

homogeneously in the whole drying process in Figure 3B, and the corresponding homogeneous shrinkage of the colloidal droplets was observed in Figure 4B, which resulted in the formation of the microbeaded PC assemblies resembling the original spherical colloidal droplets (SI, Supplementary Movie 2). With the addition of 2 vol % ethanol, the static contact angle was reduced to 138° in Figure 3C, due to the lowering of the colloidal droplet surface tension. The colloidal droplet kept a pinned TPCL during the whole evaporation process in the side-view optical images (the aqueous colloidal droplet profiles images could not provide detailed information on the TPCL movement in different directions) (Figure 3C). However, the top view optical microscopic images demonstrated asymmetric shrinkage of the colloidal droplets; that is, the droplets was pinned in one direction and shrunk in the perpendicular direction (Figure 4C and SI, Supplementary Movie 3). The asymmetric receding of the TPCL deduced from Figures 3C and 4C contributed to the formation of microellipsoidal PC assemblies.

Structures and Noniridescent Structural Colors of the Microshaped PC Assemblies. The microstructure of the PC assemblies was characterized by SEM in Figure 5. Figure 5A presents the SEM image a typical ellipsoidal assembly with an aspect ratio of 1.23 obtained by dispersing colloidal droplets with 6 vol % of ethanol on SHB substrate and drying under ambient atmosphere. The ellipsoidal PC assembly demonstrated a crack-free feature due to the use of the low-adhesive SHB substrates in Figure 5A,B.[17] Ordered, face-centered cubic, close-packed spheres with diameter of 265 nm were observed in the magnified SEM image in Figure 5C. There exited grain boundaries with sizes ranging from a few micrometers to a few

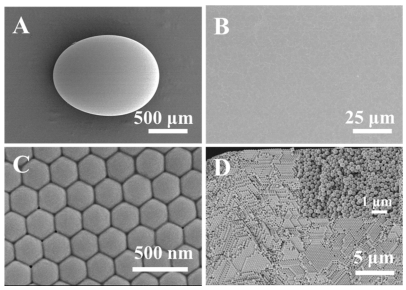

Figure 5. (A–C) Top view SEM images of the typical ellipsoidal PC assemblies with different magnifications. (D) The cross-sectional view SEM image of the surface layers of the ellipsoidal PC assemblies observed by cutting them apart with a blade. The inset SEM image presents the amorphous structure of the inner layers of the ellipsoidal PC assemblies.

dozen micrometers in the colloidal crystal region, which were more than our membrane PC films,[17] probably owing to the Gaussian curvature of the growth surface.[45] However, based on the cross-sectional images presented in Figure 5D (Figure S7, SI), the P(St-MMA-AA) spheres formed a random arrangement inside the assemblies, due to the ever-increasing Gaussian curvature of the growth surface, since the assembly happened from the droplet surface toward the inside.[28]

The existence of grain boundaries at the assembly surface layers and the amorphous arrangement inside result in the milky white appearance in Figures 1 and 2, due to the diffusive scattering of light.[46,47] To enhance the coherent structural color of the PC assemblies and eliminate the strong incoherent light-scattering, the incorporation of black substances that absorb visible light uniformly should be effective. Fe_3O_4 is a common and low-cost black substance, reflects very little light in the visible region, and is usually superparamagnetic at a domain size <30 nm.[48] Therefore, microshaped PC assemblies with enhanced structural colors were fabricated by the introduction of small amounts (2 wt % to colloidal dispersions) of Fe_3O_4 nanoparticles with an average size of 15 nm, which were synthesized by a coprecipitation method[40] and characterized by X-ray diffraction (Figure S8, SI). The introduction of the Fe_3O_4 nanoparticles had little influence on the assembly quality of the colloidal spheres due to their small particle sizes (Figure S9, SI). The optical microscopic images in Figure 6A,B (Figure S10, SI) were the PC assemblies incorporated with nanosized Fe_3O_4, which demonstrated uniform purple, green, and red structural colors, corresponding to reflectance peaks centered at 440, 563, and 679 nm in the reflectance spectra (dashed lines) of the PC assemblies in Figure 6C. The reflectance positions could be tuned by diameters of the used colloidal microspheres based on Bragg diffraction law (Figure S10, SI). Red shifts of the reflectance of the PC assemblies embedded with Fe_3O_4 nanoparticles (dashed lines) were observed and compared with the reflectance of PC assemblies without Fe_3O_4 nanoparticles (solid lines) in Figure 6C. The red shifts of the stopbands are due to the increase of the refractive index with the introduction of Fe_3O_4 nanoparticles, indicating the even dispersion of the Fe_3O_4 nanoparticles in the PC assemblies, which could be evidenced by Fe elemental mapping in Figure S11 (SI).

Importantly, the red and green structural colors of PC assemblies with shapes of microbeads and microellipsoids were independent of the view angles from 0° to 75° in Figure 6A,B observed by fixing the PC assemblies and tilting the objective lens of the digital optical microscope. The noniridescence of

DOI: 10.1021/acsami.5b07443
ACS Appl. Mater. Interfaces 2015, 7, 22644–22651

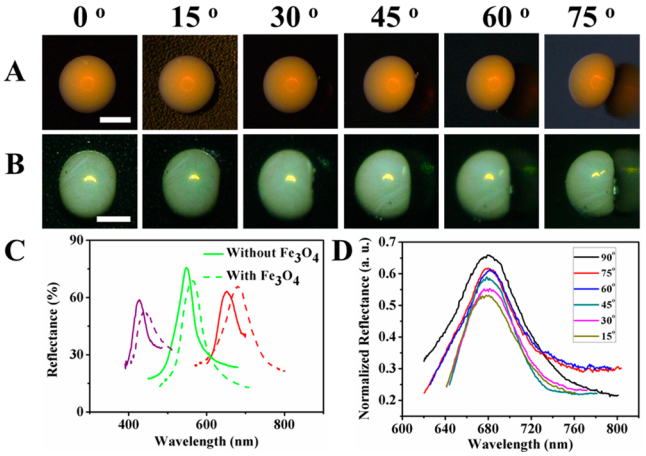

Figure 6. Digital optical microscopic images of red microbead (A) and green microellipsoid (B) PC assemblies at various viewing angles. These microshaped PC assemblies presented noniridescent structural colors independent of viewing angles. (C) The reflectance spectra of the PC assemblies with reflectance peaks centered at 427, 548, and 651 nm without Fe_3O_4 nanoparticle incorporation and 440, 563, and 679 nm with Fe_3O_4 nanoparticle incorporation. (D) The reflectance spectra of the PC assemblies recorded at various detection angles relative to the surface of the sample. The reflectance peak was independent of the incident angles, inconsistent with the observed noniridescent red structural color. Scale bar, 800 μm.

the PC assemblies was further evidenced by the unvarying reflectance peaks in the reflectance spectra at varying detection angles in Figure 6D. This noniridescent coloration is different from the iridescence coloration based on the Bragg reflection of the long-range order in the particle arrangement. Incorporation of black Fe_3O_4 nanoparticles into the periodic surface layers of the PC assemblies enhances the resonant scattering and thus suppresses iridescence.[49,50] The scattering in the photonic structures arises from Rayleigh scattering off the nanoparticle dopants or Mie scattering from lattice imperfections.[49,50] The amorphous arrangement inside the PC assemblies with only short-range orders also suppresses iridescence,[46,47,51−53] and angle-independent colors are realized by a single scattering process with wavelength-specific constructive interference.[46,47,51−53] Otherwise, the curvature of the microellipsoidal PC assemblies played a certain role in suppressing iridescence as well by inducing only small shifts of the stopbands of the ordered surface layers at varying detection angles,[36,54] which could be observed by the reflectance spectra of PC assemblies without Fe_3O_4 nanoparticle introduction (Figure S12, SI). The combination of the resonant scattering of the embedded black nanoparticles in the ordered surface layers, amorphous structures, and curvature of the PC assemblies makes them appear strongly colored, virtually independent of view angles from 0° to 75° in Figure 6A,B. Large-scale fabrication can be easily automated by continuously dispensing droplets on one side of a SHB "conveyor belt" and collecting dried assemblies on the other side. On the other hand, introduction of Fe_3O_4 nanoparticles endowed the PC assemblies with a superparamagnetic property (Figure S13, SI). The saturation magnetization of the superparamagnetic PC assemblies with imbedded 2 wt % Fe_3O_4 nanoparticles was 12.3 emu/g (Figure S13, SI). The crack-free PC assemblies with enhanced uniform noniridescent structural color and good superparamagnetism may find applications in pigments, full-color display pixels, controlled drug delivery, etc.

CONCLUSIONS

A facile approach for the controllable fabrication of noniridescent PC assemblies based on the dynamic behaviors of the TPCL of the aqueous colloidal droplets evaporating on SHB substrates was demonstrated. Continuous receding of the TPCL was proven to be responsive for the formation of the microbead PC assemblies. Receding and pinning of the TPCL in the different drying stages benefited dimpled or microwell PC assemblies, and asymmetric receding of the TPCL resulted in microellipsoidal PC assemblies. Structural characterization revealed that the PC assemblies were crack-free, consisting of ordered surface layers and amorphous inner layers. Black superparamagnetic Fe_3O_4 nanoparticles were useful to enhance the noniridescent structural colors of the PC assemblies with wide viewing angles by enhancing the resonant scattering and the single scattering process with wavelength-specific constructive interference, endowing PC assemblies with superparamagnetic property. These crack-free microshaped noniridescent PC assemblies have promising applications in nontoxic, nonbleaching pigments and energy-efficient full-color display pixels, and their facile fabrication approach developed herein may provide guidance for creating new types of substructured colloidal particles and for the control of drop shapes in inkjet printing.

ASSOCIATED CONTENT

Supporting Information

The Supporting Information is available free of charge on the ACS Publications website at DOI: 10.1021/acsami.5b07443.

SEM images, static contact angle measurement, colloid mass fraction variation during evaporation on SHB substrates, reflectance spectra, optical microscopic images, XRD pattern, Fe elemental mapping by EDS, and magnetic hysteresis loops (Figures S1−S13) and captions explaining Supplementary Movies 1−3 (PDF)

A movie showing the drying process of colloidal droplets on SHB substrates with colloidal concentration of 5 wt % (Supplementary Movie 1) (AVI)

A movie showing the drying process of colloidal droplets on SHB substrates with colloidal concentration of 40 wt % (Supplementary Movie 2) (AVI)

A movie showing the drying process of colloidal droplets on SHB substrates with colloidal concentration of 40 wt % and ethanol concentration of 2 vol % (Supplementary Movie 3) (AVI)

AUTHOR INFORMATION

Corresponding Author

*E-mail: zhoujm@iccas.ac.cn.

Notes

The authors declare no competing financial interest.

ACKNOWLEDGMENTS

This work is supported by the National Natural Science Foundation of China, Grant No. 21403052 and Hebei Natural Science Foundation, Grant No. B2015205227.

REFERENCES

(1) Yablonovitch, E. Inhibited Spontaneous Emission in Solid-state Physics and Electronics. *Phys. Rev. Lett.* **1987**, *58*, 2059−2062.

(2) John, S. Strong Localization of Photons in Certain Disordered Dielectric Superlattices. *Phys. Rev. Lett.* **1987**, *58*, 2486−2489.

DOI: 10.1021/acsami.5b07443
ACS Appl. Mater. Interfaces 2015, 7, 22644−22651

(3) Ishizaki, K.; Koumura, M.; Suzuki, K.; Gondaira, K.; Noda, S. Realization of Three-Dimensional Guiding of Photons in Photonic Crystals. *Nat. Photonics* **2013**, *7*, 133−137.
(4) Rinne, S. A.; Garcia-Santamaria, F.; Braun, P. V. Embedded Cavities and Waveguides in Three-Dimensional Silicon Photonic Crystals. *Nat. Photonics* **2008**, *2*, 52−56.
(5) Puzzo, D. P.; Arsenault, A. C.; Manners, I.; Ozin, G. A. Electroactive Inverse Opal: a Single Material for All Colors. *Angew. Chem., Int. Ed.* **2009**, *48*, 943−947.
(6) Ge, J. P.; Hu, Y. X.; Yin, Y. D. Highly Tunable Superparamagnetic Colloidal Photonic Crystals. *Angew. Chem., Int. Ed.* **2007**, *46*, 7428−7431.
(7) Hou, J.; Zhang, H. C.; Yang, Q.; Li, M. Z.; Song, Y. L.; Jiang, L. Bio-Inspired Photonic-Crystal Microchip for Fluorescent Ultratrace Detection. *Angew. Chem., Int. Ed.* **2014**, *53*, 5791−5795.
(8) Xu, X. L.; Goponenko, A. V.; Asher, S. A. Polymerized PolyHEMA Photonic Crystals: pH and Ethanol Sensor Materials. *J. Am. Chem. Soc.* **2008**, *130*, 3113−3119.
(9) Burgess, I. B.; Koay, N.; Raymond, K. P.; Kolle, M.; Lončar, M.; Aizenberg, J. Wetting in Color: Colorimetric Differentiation of Organic Liquids with High Selectivity. *ACS Nano* **2012**, *6*, 1427−1437.
(10) Xie, Z. Y.; Sun, L. G.; Han, G. Z.; Gu, Z. Z. Optical Switch of a Birefringent Photonic Crystal. *Adv. Mater.* **2008**, *20*, 3601−3604.
(11) Ge, J. P.; Goebl, J.; He, L.; Lu, Z. D.; Yin, Y. D. Rewritable Photonic Paper with Hygroscopic Salt Solution as Ink. *Adv. Mater.* **2009**, *21*, 4259−4264.
(12) Wu, S. F.; Buckley, S.; Schaibley, J. R.; Feng, L. F.; Yan, J. Q.; Mandrus, D. G.; Hatami, F.; Yao, W.; Vučković, J.; Majumdar, A.; Xu, X. D. Monolayer Semiconductor Nanocavity Lasers with Ultralow Thresholds. *Nature* **2015**, *520*, 69−72.
(13) Deotare, P. B.; Mahony, T. S.; Bulović, V. Ultracompact Low-Threshold Organic Laser. *ACS Nano* **2014**, *8*, 11080−11085.
(14) Wong, S.; Kitaev, V.; Ozin, G. A. Colloidal Crystal Films: Advances in Universality and Perfection. *J. Am. Chem. Soc.* **2003**, *125*, 15589−15598.
(15) Zhou, J. M.; Wang, J. X.; Huang, Y.; Liu, G. M.; Wang, L. B.; Chen, S. R.; Li, X. H.; Wang, D. J.; Song, Y. L.; Jiang, L. Large-area Crack-free Single-crystal Photonic Crystals via Combined Effects of Polymerization-assisted Assembly and Flexible Substrate. *NPG Asia Mater.* **2012**, *4*, e21.
(16) Hatton, B.; Mishchenko, L.; Davis, S.; Sandhage, K. H.; Aizenberg, J. Assembly of Large-Area, Highly Ordered, Crack-free Inverse Opal Films. *Proc. Natl. Acad. Sci. U. S. A.* **2010**, *107*, 10354−10359.
(17) Huang, Y.; Zhou, J. M.; Su, B.; Shi, L.; Wang, J. X.; Chen, S. R.; Wang, L. B.; Zi, J.; Song, Y. L.; Jiang, L. Colloidal Photonic Crystals with Narrow Stopbands Assembled from Low-Adhesive Superhydrophobic Substrates. *J. Am. Chem. Soc.* **2012**, *134*, 17053−17058.
(18) Velev, O. D.; Lenhoff, A. M.; Kaler, E. W. A Class of Microstructured Particles Through Colloidal Crystallization. *Science* **2000**, *287*, 2240−2243.
(19) Moon, J. H.; Yi, G. R.; Yang, S. M.; Pine, D. J.; Park, S. B. Electrospray-Assisted Fabrication of Uniform Photonic Balls. *Adv. Mater.* **2004**, *16*, 605−609.
(20) Zhao, Y. J.; Shang, L. R.; Cheng, Y.; Gu, Z. Z. Spherical Colloidal Photonic Crystals. *Acc. Chem. Res.* **2014**, *47*, 3632−3642.
(21) Xie, Z. Y.; Cao, K. D.; Zhao, Y. J.; Bai, L.; Gu, H. C.; Xu, H.; Gu, Z. Z. An Optical Nose Chip Based on Mesoporous Colloidal Photonic Crystal Beads. *Adv. Mater.* **2014**, *26*, 2413−2418.
(22) Park, J.- G.; Kim, S.- H.; Magkiriadou, S.; Choi, T. M.; Kim, Y.-S.; Manoharan, V. N. Full-Spectrum Photonic Pigments with Non-iridescent Structural Colors through Colloidal Assembly. *Angew. Chem., Int. Ed.* **2014**, *53*, 2899−2903.
(23) Teshima, M.; Seki, T.; Kawano, R.; Takeuchi, S.; Yoshioka, S.; Takeoka, Y. Preparation of Structurally Colored, Monodisperse Spherical Assemblies Composed of Black and White Colloidal Particles Using a Micro-Flow-Focusing Device. *J. Mater. Chem. C* **2015**, *3*, 769−777.
(24) Takeoka, Y.; Yoshioka, S.; Teshima, M.; Takano, A.; Harun-Ur-Rashid, M.; Seki, T. Structurally Coloured Secondary Particles Composed of Black and White Colloidal Particles. *Sci. Rep.* **2013**, *3*, 2371.
(25) Kim, S.- H.; Lim, J.- M.; Jeong, W. C.; Choi, D.- G.; Yang, S.-M. Patterned Colloidal Photonic Domes and Balls Derived from Viscous Photocurable Suspensions. *Adv. Mater.* **2008**, *20*, 3211−3217.
(26) Rastogi, V.; Melle, S.; Calderón, O. G.; García, A. A.; Marquez, M.; Velev, O. D. Synthesis of Light-Diffracting Assemblies from Microspheres and Nanoparticles in Droplets on a Superhydrophobic Surface. *Adv. Mater.* **2008**, *20*, 4263−4268.
(27) Millman, J. R.; Bhatt, K. H.; Prevo, B. G.; Velev, O. D. Anisotropic Particle Synthesis in Dielectrophoretically Controlled Microdroplet Reactors. *Nat. Mater.* **2005**, *4*, 98−102.
(28) Rastogi, V.; García, A. A.; Marquez, M.; Velev, O. D. Anisotropic Particle Synthesis Inside Droplet Templates on Superhydrophobic Surfaces. *Macromol. Rapid Commun.* **2010**, *31*, 190−195.
(29) Sperling, M.; Velev, O. D.; Gradzielski, M. Controlling the Shape of Evaporating Droplets by Ionic Strength: Formation of Highly Anisometric Silica Supraparticles. *Angew. Chem., Int. Ed.* **2014**, *53*, 586−590.
(30) Lim, C. H.; Kang, H.; Kim, S.- H. Colloidal Assembly in Leidenfrost Drops for Noniridescent Structural Color Pigments. *Langmuir* **2014**, *30*, 8350−8356.
(31) Cai, J. H.; Chen, S. R.; Cui, L. Y.; Chen, C. C.; Su, B.; Dong, X.; Chen, P. L.; Wang, J. X.; Wang, D. J.; Song, Y. L.; Jiang, L. Tailored Porphyrin Assembly at the Oil−Aqueous Interface Based on the Receding of Three-Phase Contact Line of Droplet Template. *Adv. Mater. Interfaces* **2015**, *2*, 1400365.
(32) Wang, T.; Chen, S. R.; Jin, F.; Cai, J. H.; Cui, L. Y.; Zheng, Y. M.; Wang, J. X.; Song, Y. L.; Jiang, L. Droplet-assisted Fabrication of Colloidal Crystals from Flower-shaped Porphyrin Janus Particles. *Chem. Commun.* **2015**, *51*, 1367−1370.
(33) Cai, J. H.; Wang, T.; Wang, J. X.; Song, Y. L.; Jiang, L. Temperature-controlled Morphology Evolution of Porphyrin Nanostructures at an Oil−Aqueous Interface. *J. Mater. Chem. C* **2015**, *3*, 2445−2449.
(34) Deegan, R. D.; Bakajin, O.; Dupont, T. F.; Huber, G.; Nagel, S. R.; Witten, T. A. Capillary Flow as the Cause of Ring Stains from Dried Liquid Drops. *Nature* **1997**, *389*, 827−829.
(35) Marína, Á. G.; Gelderblom, H.; Susarrey-Arce, A.; van Houselt, A.; Lefferts, L.; Gardeniers, J. G. E.; Lohse, D.; Snoeijer, J. H. Building Microscopic Soccer Balls with Evaporating Colloidal Fakir Drops. *Proc. Natl. Acad. Sci. U.S.A.* **2012**, *109*, 16455−16458.
(36) Kuang, M. X.; Wang, J. X.; Bao, B.; Li, F. Y.; Jiang, L.; Song, Y. L. Inkjet Printing Patterned Photonic Crystal Domes for Wide Viewing-Angle Displays by Controlling the Sliding Three Phase Contact Line. *Adv. Opt. Mater.* **2014**, *2*, 34−38.
(37) Kuncicky, D. M.; Bose, K.; Costa, K. D.; Velev, O. D. Sessile Droplet Templating of Miniature Porous Hemispheres from Colloid Crystals. *Chem. Mater.* **2007**, *19*, 141−143.
(38) Wang, J. X.; Wen, Y. Q.; Ge, H. L.; Sun, Z. W.; Zheng, Y. M.; Song, Y. L.; Jiang, L. Simple Fabrication of Full Color Colloidal Crystal Films with Tough Mechanical Strength. *Macromol. Chem. Phys.* **2006**, *207*, 596−604.
(39) Su, B.; Li, M.; Lu, Q. H. Toward Understanding Whether Superhydrophobic Surfaces Can Really Decrease Fluidic Friction Drag. *Langmuir* **2010**, *26*, 6048−6052.
(40) Baumgartner, J.; Dey, A.; Bomans, P. H. H.; Le Coadou, C.; Fratzl, P.; Sommerdijk, N. A. J. M.; Faivre, D. Nucleation and Growth of Magnetite from Solution. *Nat. Mater.* **2013**, *12*, 310−314.
(41) Zhang, Y.- L.; Xia, H.; Kim, E. Y.; Sun, H.- B. Recent Developments in Superhydrophobic Surfaces with Unique Structural and Functional Properties. *Soft Matter* **2012**, *8*, 11217−11231.
(42) McGrath, J. G.; Bock, R. D.; Cathcart, J. M.; Lyon, L. A. Self-Assembly of "Paint-on" Colloidal Crystals Using Poly (styrene-co-*N*-isopropylacrylamide) Spheres. *Chem. Mater.* **2007**, *19*, 1584−1591.
(43) Cui, L. Y.; Li, Y. F.; Wang, J. X.; Tian, E. T.; Zhang, X. Y.; Zhang, Y. Z.; Song, Y. L.; Jiang, L. Fabrication of Large-Area Patterned

DOI: 10.1021/acsami.5b07443
ACS Appl. Mater. Interfaces 2015, 7, 22644−22651

Photonic Crystals by Ink-jet Printing. *J. Mater. Chem.* **2009**, *19*, 5499−5502.
(44) Ramos, S. M. M.; Dias, J. F.; Canut, B. Drop Evaporation on Superhydrophobic PTFE Surfaces Driven by Contact Line Dynamics. *J. Colloid Interface Sci.* **2015**, *440*, 133−139.
(45) Meng, G. N.; Paulose, J.; Nelson, D. R.; Manoharan, V. N. Elastic Instability of a Crystal Growing on a Curved Surface. *Science* **2014**, *343*, 634−637.
(46) Takeoka, Y.; Yoshioka, S.; Takano, A.; Arai, S.; Nueangnoraj, K.; Nishihara, H.; Teshima, M.; Ohtsuka, Y.; Seki, T. Production of Colored Pigments with Amorphous Arrays of Black and White Colloidal Particles. *Angew. Chem., Int. Ed.* **2013**, *52*, 7261−7265.
(47) Takeoka, Y. Angle-Independent Structural Coloured Amorphous Arrays. *J. Mater. Chem.* **2012**, *22*, 23299−23309.
(48) Ge, J. P.; Hu, Y. X.; Biasini, M.; Beyermann, W. P.; Yin, Y. D. Superparamagnetic Magnetite Colloidal Nanocrystal Clusters. *Angew. Chem., Int. Ed.* **2007**, *46*, 4342−4345.
(49) Pursiainen, O. L. J.; Baumberg, J. J.; Winkler, H.; Viel, B.; Spahn, P.; Ruhl, T. Nanoparticle-Tuned Structural Color from Polymer Opals. *Opt. Express* **2007**, *15*, 9553−9561.
(50) Aguirre, C. I.; Reguera, E.; Stein, A. Colloidal Photonic Crystal Pigments with Low Angle Dependence. *ACS Appl. Mater. Interfaces* **2010**, *2*, 3257−3262.
(51) Zhang, Y. F.; Dong, B. Q.; Chen, A.; Liu, X. H.; Shi, L.; Zi, J. Using Cuttlefish Ink as an Additive to Produce Non-iridescent Structural Colors of High Color Visibility. *Adv. Mater.* **2015**, *27*, 4719−4724.
(52) Rockstuhl, C.; Lederer, F. Suppression of the Local Density of States in a Medium Made of Randomly Arranged Dielectric Spheres. *Phys. Rev. B* **2009**, *79*, 132202.
(53) Liew, S. F.; Yang, J.-K.; Noh, H.; Schreck, C. F.; Dufresne, E. R.; O'Hern, C. S.; Cao, H. Photonic Band Gaps in Three-Dimensional Network Structures with Short-Range Order. *Phys. Rev. A* **2011**, *84*, 063818.
(54) Gu, H. C.; Zhao, Y. J.; Cheng, Y.; Xie, Z. Y.; Rong, F.; Li, J. Q.; Wang, B. P.; Fu, D. G.; Gu, Z. Z. Tailoring Colloidal Photonic Crystals with Wide Viewing Angles. *Small* **2013**, *9*, 2266−2271.

DOI: 10.1021/acsami.5b07443
ACS Appl. Mater. Interfaces 2015, 7, 22644−22651